Life Sciences 234 (2019) 116783

Contents lists available at ScienceDirect

Life Sciences

journal homepage: www.elsevier.com/locate/lifescie

Bulbine frutescens phytochemical inhibits notch signaling pathway and induces apoptosis in triple negative and luminal breast cancer cells

Prem Prakash Kushwaha[a], Pothabathula Sheshu Vardhan[a], Petrina Kapewangolo[b], Mohammad Shuaib[a], Sunita Kumari Prajapati[a], Atul Kumar Singh[a], Shashank Kumar[a,*]

[a] Department of Biochemistry and Microbial Sciences, Central University of Punjab, Bathinda 151001, Punjab, India
[b] Department of Chemistry and Biochemistry, Faculty of Science, University of Namibia, P/Bag 13301, Windhoek, Namibia

ARTICLE INFO

Keywords:
Breast cancer
Bulbine frutescens
Notch signaling
Apoptosis
Natural products
Anticancer

ABSTRACT

Breast cancer (BCa) is the most commonly diagnosed lethal cancer in women worldwide. Notch signaling pathway is directly linked to BCa recurrence and aggressiveness. Natural remedies are becoming a prime choice to overcome against cancer due to lesser side effect and cost-effectiveness. *Bulbine frutescens* (Asphodelaceae), a traditional medicinal plant in South Africa possess bioactive flavonoids and terpenoids. Polar (methanol) and non-polar (hexane) *B. frutescens* plant extracts were prepared. GC–MS analysis revealed the differential presence of secondary metabolites in both methanolic and hexane extracts. We hereby first time evaluated the anticancer potential of *B. frutescens* methanolic and hexane extract in triple-negative and luminal BCa cells. *B. frutescens* extracts significantly decreased cell viability (IC_{50} 4.8–28.4 μg/ml) and induced cell cycle arrest at G_1 phase in MDA-MB-231 and T47D cells as confirmed by spectrophotometry and flow cytometry technique. RT-PCR analysis of cell cycle (cyclin D1, CDK4, and p21) and apoptosis modulating genes (caspase 3, Bcl2 and survivin) revealed upexpression of p21, and caspase 3, and down expression of cyclin D1, CDK4, Bcl2 and survivin genes in extract-treated BCa cells. Fluorescence spectrophotometry and confocal microscopy showed *B. frutescens* induced nuclear morphology and mitochondrial integrity disruption, and increased reactive oxygen species production in MDA-MB-231 and T47D cells. Flow cytometric apoptosis analysis of *B. frutescens* extracts treated MDA-MB-231 cells showed ≈13% increase in early apoptotic population in comparison to non-treated cells. Dual-Luciferase Reporter assay confirmed notch promoter inhibitory activity of *B. frutescens* extracts. Moreover, RTPCR analysis showed down regulation of notch responsive genes (Hes1 and Hey1) at transcription levels in extract-treated BCa cells. Western Blot analysis showed increased procaspase 3 protein expression in extract-treated BCa cells. In all the assays methanolic extract showed better anti-cancer properties. Literature-based identification of methanol soluble phytochemicals in *B. frutescens* and in silico docking study revealed Bulbineloneside D as a potent ϒ-secretase enzyme inhibitor. In comparison to standard notch inhibitor, lead phytochemical showed two additional hydrophobic interactions with Ala80 and Leu81 amino acids. In conclusion, *B. frutescens* phytochemicals have cell cycle arrest, ROS production, apoptosis induction, and mitochondria membrane potential disruption efficacy in breast cancer cells. *B. frutescens* phytochemicals have the ability to downregulate the notch signaling pathway in triple-negative and luminal breast cancer cells.

1. Introduction

Breast cancer (BCa) is the second most common cancer throughout the world both in incidence and death. It accounts for 14% of total cancer in India and causes major mortality among women. In 2018, around 1.5 lakh new BCa cases were diagnosed and 0.9 lakh deaths occurred due to this cancer in India [1]. Different subtypes of breast cancer show differential drug susceptibility, prognosis, and aggressiveness. Triple-negative breast cancer (TNBC) is more aggressive in nature, susceptible to chemotherapy and show poor prognosis. On the other hand, luminal type of BCa cells are less drug-susceptible, show better prognosis and are comparatively less aggressive in nature. Hormonal, chemo, and radiotherapy are frequently used to treat breast cancer, diminish recurrence, and prevent tumor growth. Regrettably, sometimes therapy outcomes showed adverse effects or become resistant. Natural drugs are of choice nowadays in anticancer drug discovery due to their lesser side effect and cost-effectiveness [2–3]. Thus, there is an urgent need to find some natural anticancer agents with lesser side effect and cost-effective.

* Corresponding author.
E-mail address: shashank.kumar@cup.edu.in (S. Kumar).

https://doi.org/10.1016/j.lfs.2019.116783

Available online 21 August 2019

Notch signaling cascade plays an important role in BCa progression, aggressiveness and drug resistance [4–5]. Notch receptor-ligand interaction initiates the signaling with the help of membrane-bound ϒ-secretase enzyme complex. The enzyme cleaves the intracellular domain of the notch receptor-ligand complex and produces notch intracellular cellular domain (NICD). Cytoplasmic NICD translocate into the nucleus, activate transcription of notch targeted genes by deactivating the transcription repressor complex on notch promoter. Upregulation of notch targeted genes (Hes1 and Hey1) is associated with cell cycle checkpoint skip and increased expression of anti-apoptotic proteins in breast cancer cells [6–8]. Production of excessive free radicals (reactive oxygen species-ROS) in cancer cells is one of the important strategies to kill cancer cells. Drug-induced excessive ROS production in cancer cells damage mitochondria by disrupting mitochondrial membrane potential. Recently notch signaling pathway is reported to involve in the maintenance of mitochondria membrane potential [9].

Bulbine frutescens (Asphodelaceae) is commonly used as a traditional medicinal plant in South Africa for the treatment of skin wounds and burns [10]. Very few literatures are available on *B. frutescens* which generally include phytochemical isolation and preliminary screening of biological activity of the plant. *B. frutescens* aqueous extract increases glucose utilization potential in vitro [11]. Isofuranonapthoquinone 1, isolated from *B. frutescens* is an inhibitor of Glutathione transferase P1-1 (GSTP1-1) protein [12]. Besides, HIV-1 protease inhibition by aqueous and ethanolic extracts of Bulbine genus potentiates the medicinal property of the plant. Literature shows lacuna regarding studies on evaluation of the anticancer potential of *B. frutescens* plant extracts and its underlying mechanism. Thus, we hereby designed the first study to establish *B. frutescens* extract anticancer mode of action in breast cancer cells. Moreover, identification of phytochemicals present in methanolic and hexane extract was carried out by using GC–MS technique.

2. Methodology

2.1. Reagents

Dulbecco's modified eagle medium (DMEM), fetal bovine serum (FBS), trypsin, penicillin, streptomycin, JC-1 (5,5′,6,6′-tetrachloro-1,1′,3,3′-tetraethylbenzimi-dazolylcarbocyanine iodide), 2′,7′-dichlorodihydrofluorescein diacetate (H2DCFDA), annexin V fluorescein Isothiocyanate (annexin V FITC), Hoechst 33342, RNAase A, trizol, and lipofectamine 3000 were from Thermo Fisher Scientific, USA. MTT (3-(4,5-dimethylthiazol-2-yl)-2,5-diphenyl tetrazolium bromide) was obtained from Sigma-Aldrich, USA. The iScript™ cDNA synthesis kit and SYBR® green master mix were purchased from Biorad, USA. Propidium iodide (PI) and primers were purchased from Abcam, UK and GCC biotech, India respectively. Luciferase/Renilla vector and dual-luciferase reporter assay system were procured form Promega Corporation, USA. Caspase 3 primary antibody (Cat: ab32351) and β-actin secondary antibody (Cat: 4970S) was purchased from Abcam, UK, and Imperial Life Sciences, India respectively.

2.2. Plant material and extraction

Fresh plant samples (bulb) of *Bulbine frutescens* were obtained from “Farm Vredelus” in 2018. Farm Vredelus is a farm located in Mariental, Namibia, that grows medicinal plants. The plant was authenticated by Silke Rugheimer at the National Herbarium of Namibia; voucher specimen number M2. Collected samples (bulb) were washed, sterilized (wiped with ethanol), and extracted in hexane and methanol separately for 48 h. The bulb was extracted fresh. It takes very long to dry because of its high water content. The semi-solid extract was further dried by using rotary evaporator and stored until further use.

2.3. GC–MS analysis

Secondary metabolites present in the *B. frutescens* methanolic (BME) and hexane extract (BHE) were identified by using Gas-Chromatography coupled with Mass Spectroscopy (GC–MS) technique. Respective dried extracts were dissolved in 100% methanol and hexane for the analysis. The GC–MS analysis was performed using Shimadzu QP 2010 Ultra-Mass Spectrometer equipped with an integrated chromatograph with an RTXi-5MS column. The ion source temperature was 200 °C and the interface temperature was 260 °C. The data was acquired using a mass detector from 5 min of the sample injection. Pressure mode at 66.7 kPa controlled the flow of the sample. The total flow and column flow rate were 10.4 ml/min and 1.24 ml/min respectively. The maintenance of the split ratio was at 5:0. The column injector temperature was 250 °C and the column oven temperature was maintained for 10 min at 280 °C. Dissolved samples had been delivered via injector running within the split mode with helium gas. The identity of phytoconstituents became completed with the aid of evaluation of retention time and fragmentation pattern with mass spectra inside the NIST11.0 spectral library. The chromatogram was processed by using GC–MS Real-Time Analysis Software version 1.10 beta.

2.4. Cell culture

Human breast cancer cells (MDA-MB-231 and T47D) and human embryonic kidney 293 (HEK293) cells were purchased from National Centre for Cell Sciences, Pune. These cells were cultured in Dulbecco's Modified Eagle Medium (DMEM) supplemented with 10% (*v*/v) heat-inactivated FBS, 2 mM L-glutamine, 100 U/ml of penicillin, and 100 µg/ml of streptomycin. Cells were maintained at 37 °C under a humid environment in an incubator having 5% CO_2.

2.5. MTT assay

The effect of *B. frutescens* methanol extract (BME) and *B. frutescens* hexane extract (BHE) on cell viability was measured by MTT assay following the method by Mosmann et al. [13]. Briefly, the cells (1×10^4 cells/well) were seeded in a 96 well microtiter plate (100 µl/well) in triplicate. BME and BHE treatment were done for 24, 48 and 72 h at different concentrations (10, 30, 50, 70, and 100 µg/ml). After incubation, 10 µl of MTT solution (5 mg/ml) was added to each well and incubated for 4 h at 37 °C. Formazan crystals were solubilized with 100 µl dimethyl sulfoxide (DMSO) and the absorbance was measured at 590 nm using a microplate reader (BioTek Instruments, Inc. USA). The IC_{50} value was calculated for cell viability.

2.6. Measurement of mitochondrial membrane potential (ΔΨm)

The fluorescent dye JC-1 accumulates in the mitochondrial matrix. Mitochondrial membrane potential (ΔΨm) is responsible for the structural integrity of mitochondria. At high ΔΨm, JC-1 forms aggregates in the mitochondria that exhibit red fluorescence. At lower ΔΨm, a lower quantity of the dye could enter into the mitochondria, no aggregates could be found and the dye maintains its monomeric form resulting in green fluorescence [14]. MDA-MB-231 and T47D breast cells (3×10^3 cells/well) were seeded in a 96 well microtiter plate (100 µl/well) in triplicates. Cells were treated for 48 h at IC_{50} concentration of BME and BHE. After incubation, 100 µl of JC-1 dye solution (2 µM) was added to each well and incubated for 30 min at 37 °C. The absorbance was measured at excitation/emission wavelength of 529/590 nm using a microplate reader.

2.7. Determination of intracellular reactive oxygen species (ROS)

The levels of ROS were determined quantitatively by using 2, 7-dichlorodihydrofluorescein diacetate (DCFH-DA) dye [15]. Briefly,

MDA-MB-231 and T47D cells (3×10^3 cells/well) were plated in the 96-well tissue culture media containing 10% FBS and 1% penicillin/streptomycin and incubated at 37 °C with 5% CO_2 overnight. The cells were treated for 48 h at IC_{50} concentration of BME and BHE. The supernatants were removed, and attached cells were washed with PBS. The cells were further incubated for 4 h after re-suspending in 100 µl H2DCFDA dye solution (20 µM). Subsequently, the fluorescence intensity was measured at an excitation/emission wavelength of 495/530 nm using a fluorescence microplate reader.

2.8. Cell cycle analysis by flow cytometer

MDA-MB-231 and T47D cells (1×10 [5]) were seeded into 6-well plate followed by treatment with BME and BHE (at IC_{50}) after 24 h. The cells were further incubated for 24 h, and 48 h. After incubation, cells were detached and fixed with 500 µl of 70% ethanol at −20 °C for 2 h. Subsequently, the cells were washed thrice with 1 ml of PBS (pH 7.4). Cells were finally re-suspended in 1 ml of PBS containing 0.1% triton X, 10 mM EDTA, 50 mg/ml RNase A and 2 mg/ml PI. The cells were analyzed by a flow cytometer (BD Accuri) [16].

2.9. Flow cytometric apoptotic cell death analysis by annexin V FITC-PI staining

Flow cytometric technique was used to quantify the BME and BHE induced apoptotic cell death in breast cancer cells. Briefly, 1×10^5 breast cancer cells (MDA-MB-231) were seeded in 35 mm treated culture dishes containing 1 ml of culture media. The cells were treated with BME and BHE for 12 h at sub IC_{50} and IC_{50} concentrations. After incubation, cells were trypsinized and washed twice with cold PBS. The cells were resuspended in 100 µl annexin binding buffer containing annexin V FITC and PI and further incubated for 15 min at room temperature in the dark. Additionally, 400 µl annexin binding buffer was added and immediately analyzed through flow cytometer (BD Accuri C6) [17].

2.10. Notch promoter assay

Dual-luciferase assay technique is used to asses notch promoter activity. In this assay, we used pGL4[luc2P/RBP-JK-RE/Hygro] vector having NICD binding site (notch promoter) fused with luciferase gene. p [Rluc-Neo/SV40] vector (*Renilla*) was used as an internal control. HEK293 cells (4×10^4 cells/well) were seeded in a 96-well plate. The cells were transfected with pGL4[luc2P/RBP-JK-RE/Hygro] and p [Rluc-Neo/SV40] vectors using Lipofectamine 3000 transfection reagent (Thermo Fisher Scientific, Waltham, MA, USA) according to the manufacturer's guidelines. Transfected cells were treated with extracts (IC_{50}) and DAPT (20 µM). The plate was further incubated for 24 h at 37 °C. The Luciferase activity was measured by using Dual-Luciferase Reporter Assay Kit (Promega Corporation, USA) on GloMax 20/20 Luminometer (Promega Corporation, USA).

2.11. Total RNA isolation, cDNA synthesis, and quantitative RT-PCR

One million cells/well were plated into the six-well plates in culture media supplemented with 10% FBS and 1% penicillin/streptomycin and incubated at 37 °C. Cells were exposed to BME and BHE treatment at IC_{50} concentration for 24, and 48 h. Total RNA was extracted using Trizol (Thermo Scientific Fisher) solution according to the manufacturer's instruction. RNA was quantified at 260/280 nm using Thermo Scientific Nanodrop 2000 Spectrophotometer. The absorption ratio (A260 nm/A280 nm) between 1.90 and 2 was taken into consideration for cDNA preparation. Approximately one microgram of total RNA was reverse transcribed into cDNA using a high capacity iScript™ cDNA Synthesis Kit (BIORAD). mRNA expression was quantified by RT-PCR by using Veriti® 96-well fast thermal cycler (Applied Biosystems). The following cycling parameters were optimized as follows: start at 95 °C for 5 min, denaturing at 95 °C for 30 s, annealing at 55 °C for 45 s, elongation at 72 °C for 45 s, and a final 5 min extra extension at the end of the reaction to ensure that all amplicons were completely extended and repeated for 40 amplification cycles [18]. GAPDH was used as a housekeeping gene to assure equal loading of the sample. List and sequence of primers are given in Table S1 in supplemental materials.

2.12. Western blot analysis

Western blot technique was used to detect the protein expression levels in breast cancer cells. The cells were seeded at the density of 2×10^5 cells/well in a 6-well plate and incubated overnight for attachment followed by treatment with *B. frutescens* extracts for 12 h at IC_{50} concentration. Subsequently, the treated cells were detached and harvested in RIPA buffer followed by 30 min incubation on ice and centrifuged at 10,000 × *g* for 15 min. Bicinchoninic acid assay (BCA) protein quantitation reagent kit (Thermo Fisher Scientific) was used to estimate the protein content present in the lysate. The 2X SDS-PAGE loading buffer (200 mM DTT, 100 mM Tris-HCl (pH 6.8), 0.1 bromophenol blue, 4% SDS, and 20% glycerol) was used to load the sample on the gel. An equal amount of total protein and loading buffer was taken and boiled for 10 min before loading. The protein sample was electrophoresed in the tris-glycine electrophoresis buffer [250 mM glycine, 25 mM Tris-HCl (pH 8.3), and 0.1% SDS] at 100 V for 1.5 h. The separated proteins were blotted on the PVDF membrane with transfer buffer (25 mM Tris, 20% methanol, 0.04% SDS and 192 mM glycine) for 2 h. The 5% non-fat milk in TBST [150 mM NaCl, 20 mM Tris-HCl (pH 7.4) and 0.1% (*v*/v) Tween-20] was used to block the membrane for 2 h at room temperature. The blotted membrane was incubated with primary antibody at 4 °C overnight followed by TBST wash thrice (10 min interval each). Horseradish peroxidase-conjugated secondary antibody was diluted in blocking buffer for 2 h at room temperature followed by three wash with TBST for 10 min. The blots were developed with the enhanced chemiluminescence (ECL) system (Thermo Fisher Scientific). The image was captured using image lab software 6.0.1 Bio-Rad.

2.13. Confocal microscopy

2.13.1. Nucleus staining by Hoechst 33342 dye

MDA-MB-231 and T47D cells at a density of 2×10^4 cells/well were seeded in 24-well plates, and after incubation for 24 h, fresh culture media containing BME and BHE at IC_{50} concentration were added and incubated in a humidified incubator at 37 °C for 16 h. After incubation, the cells were stained with Hoechst 33342 dye (5 µg/ml) in culture medium at room temperature in the dark for 20 min. Subsequently, the cells were washed twice with PBS and immediately evaluated by a confocal microscope.

2.13.2. Mitochondrial live/dead analysis using JC-1 dye

MDA-MB-231 and T47D cells were placed in 6-well plates and cultured overnight. Then, MDA-MB-231 and T47D cells were cultured in the medium with BME and BHE at IC_{50} concentration for 16 h. After that, MDA-MB-231 and T47D cells were stained with 5 µM JC-1 dye for 20 min at 37 °C in the dark. Mitochondrial membrane potential depletion was observed under a confocal microscope.

2.13.3. ROS generation analysis using H2-DCFDA dye

For reactive oxygen species analysis, 0.2×10^6 cells were plated in 6 well plates in DMEM. After 24 h, MDA-MB-231 and T47D cells were treated with BME and BHE at IC_{50} concentration for the next 16 h. After that, MDA-MB-231 and T47D cells were stained with 1 µM H2-DCFDA for 20 min at 37 °C in the dark. Then ROS production levels were observed under a confocal microscope.

2.14. Literature-based identification and in silico screening of potential notch inhibitor from B. frutescens

Different search engines such as Google Scholar, PubMed, Scopus were used for the survey of methanol soluble phytochemicals present in *B. frutescens* plant. Crystal structure of γ-secretase (PDB ID: 4Y6K) was downloaded from the RCSB protein data bank (http://www.rcsb.org/). Missing side chains, bond order assignment, and hydrogen bond optimization in all the proteins were carried out by using a protein preparation module of the Schrödinger suite v9.2. Grids for all the proteins were prepared by selecting the corresponding co-crystallized ligands. Phytochemical presets in the *B. frutescens* methanolic extracts were drawn using ChemSketch and prepared using the ligprep module. Phytochemicals were docked with ϒ-secretase protein using Glide extra precision (XP) module, to understand their interactions and binding efficacy with the target protein. Pymol software was used for visualization of the interaction pattern in the protein-ligand complex.

2.15. Statistical analysis

All data are presented as the mean ± standard deviation of at least three independent experiments. All statistical analyses were performed using GraphPad Prism 5.0 version software (GraphPad Software, San Diego, California). Statistical comparisons between the control and treatments were performed using one-way analysis of variance. $P < 0.05$ was considered to indicate a statistically significant difference.

3. Results

3.1. GC–MS analysis

GC–MS analysis of *B. frutescens* methanolic and hexane extract showed the occurrence of various secondary metabolites (Fig. 1A–B). Hexane extract showed comparatively greater number of phytochemicals ($n = 103$) than methanolic extract ($n = 25$). Name of identified compounds, their molecular formula, molecular weight, retention time and peak area are given in Table S2 in supplemental materials. In hexane extract, tritetracontane; urs-12-ene; 1,1,6-trimethyl-3-methylene-2-(3,6,1013,14-pentamethyl-3-ethenyl-pentadec-4-enye)cyclohexane; docosane, 2,4-dimethy; phthalic acid, bis(7-methyloctyl) ester; bis(tridecyl) phthalate; terephthalic acid, dodecyl 2-ethylhexy ester; 1-

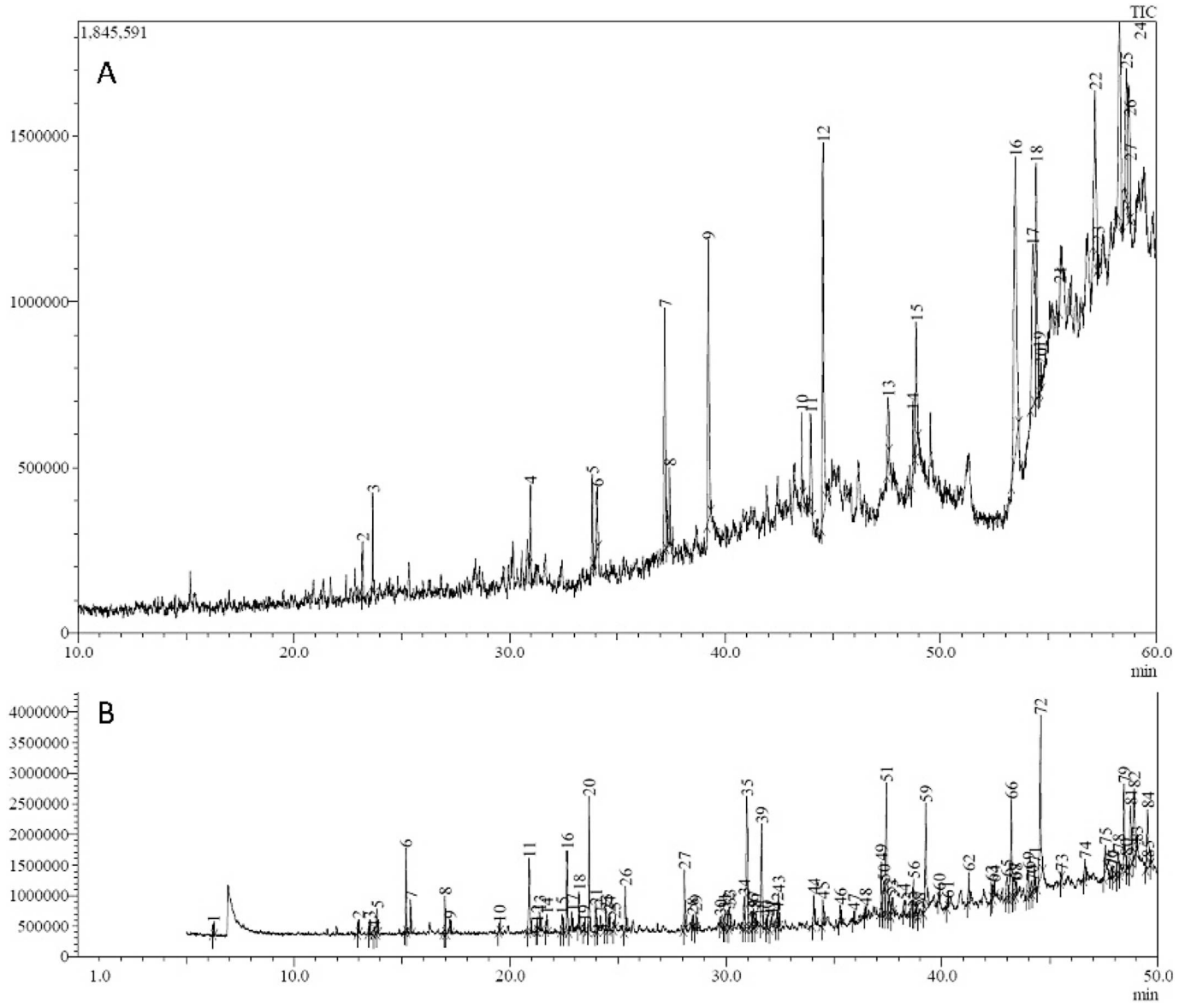

Fig. 1. GCMS chromatograph of *B. frutescens* (A) methanolic and (B) hexane extract.

nonene, 4,6,8-trimethyl; 9-octadecenamide; 2H-pyran-2-carboxylic acid, 3,6-dihydro-6-methoxy-, ethyl ester; 9,12,15-octadecatrienoic acid, 2-[(trimethylsilyl)oxy]-1-[[(trimethylsilyl)oxy]methyl]ethyl ester (Z,Z,Z); indan-1,3-diol monoacetate; nonane, 5-(1-methylpropyl); 6,10,14,18,22-tetracosapentaen-2-ol; bis(tridecyl) phthalate and 1,2-Benzenedicarboxylic acid, dinonyl ester compounds showed > 1% peak area. In methanolic extract, 2-propenoic acid, pentadecyl ester; tetradecanoic acid; n-hexadecanoic acid; 9-octadecenal; heptadecane; heptadecane, 2-methyl; tritetracontane; Z-11-pentadecenol; 2-methyloctacosane; 2,6,10,14,18-pentamethyl-2,6,10,14,18-eicosapentaene; and 1,2-octadecanediol showed > 1% peak area (Table S2 in supplemental materials).

3.2. B. frutescens extracts inhibit MDA-MB-231 and T47D human breast cancer cellular proliferation

Polar (methanol) and non-polar (hexane) extracts of *B. frutescens* were tested for their potential to inhibit the MDA-MB-231 and T47D cell lines using MTT assay. The experiment was used to find a basis for the characterization of *B. frutescens* extracts induced a cellular response in two different breast cancer cell line models. Dose- and time-dependent antiproliferative property of BME and BHE extract was found in MDA-MB-231 and T47D cell lines (Fig. 2A–D). BME extract showed ≈53% inhibition in MDA-MB-231 and T47D cell lines at 10 μg/ml concentration in 24 h treatment. BHE extract showed about 75% and 63% inhibition in MDA-MB-231 and T47D cell lines respectively at 10 μg/ml concentration in 24 h. BHE extract showed similar efficacy (about 33–37% viability) at higher concentration (70 and 100 μg/ml) in MDA-MB-231 cells in 48 h and 72 h. At 100 μg/ml concentration BHE extract show comparatively lesser cell viability in T47D cells in 72 h. Approximately similar patterns of cell viability were observed in the presence of the BME extract in MDA-MB-231 and T47D cell lines at 100 μg/ml in 72 h.

IC_{50} value calculation and regression analysis were done using GraphPad Prism software to study the effect of BME and BHE extract treatment in MDA-MB-231 and T47D cells in 24 h, 48 h and 72 h treatment (Fig. 2E–P). The calculations were based on the MTT results obtained after the test extract treatment in MDA-MB-231 and T47D cells at a different time interval. BME and BHE extract showed 4.877 μg and 13.12 μg IC_{50} value in MDA-MB-231 cells in the initial 24 h treatment. Similarly, BME and BHE extract showed 6.35 μg and 12.08 μg IC_{50} value in T47D cells in the initial 24 h treatment (Fig. 2). Regression analysis of different experimental setup showed the R^2 values in the range of 0.9119–0.9916.

3.3. B. frutescens extracts arrest cell cycle in the G1 phase in MDA-MB-231 and T47D breast cancer cells

To understand the underlying mechanism of BME and BHE extract induced cell proliferation we studied the cell cycle distribution in the MDA-MB-231 (ER^-/PR^- breast cancer cell model) and T47D breast cancer cells (ER^+/PR^+ breast cancer cell model). Untreated T47D cancer cells showed 42.33, 8.53 and 21.57% cells distribution in G1, S and G2/M phase of cell cycle respectively (Fig. 3A′ and D′). BME treated T47D cells showed increased levels of G1 cell populations, both in 24 h (54.7%) and 48 h (51.3%) of the treatment (Fig. 3B′). Treatment of T47D cells with the BHE extract also showed the similar efficacy of cell cycle arrest in the G1 phase in 24 h (55%) and 48 h (58%) of the treatment (Fig. 3F′). It should be noted that BHE extract showed better cell cycle G1 phase arrest (58%) in the ER^+/PR^+ breast cancer cell line in 48 h treatment (Fig. 3G′). BME treated MDA-MB-231 cells showed increased levels of G1 cell populations, both in 24 h (47%) and 48 h (42.33%) of the treatment (Fig. 3D). Treatment of MDA-MB-231 cells with the BHE extract also showed cell cycle arrest potential in the G1 phase in 24 h (46%) and 48 h (39%) of the treatment. It should be noted that BHE extract showed better cell cycle G1 phase arrest (58%) in the ER^-/PR^- breast cancer cell line in 24 h treatment (Fig. 3C).

3.4. B. frutescens extracts decrease cyclin D1 and CDK4 mRNA levels in breast cells

To understand the underlying mechanism of BME and BHE extract induced cell cycle arrest in MDA-MB-231 (ER^-/PR^- breast cancer cell model) and T47D (ER^+/PR^+ breast cancer cell model) breast cancer cells, we examined the mRNA levels of cyclin D1 and CDK4. Interaction of cyclin D1 with cyclin dependent kinases (CDK4/6) induces expression of genes involved in G1-S phase transition and promotes cellular proliferation. BME treatment (24 h) significantly reduced the cyclin D1 and CDK4 mRNA levels in MDA-MB-231 and T47D cells (Fig. 4A–B). BME extract significantly reduced cyclin D1 mRNA levels in MDA-MB-231 and T47D cancer cells in 24 h treatment (Fig. 4B). In comparison to BME extract, BHE treatment showed less potential to decrease mRNA levels of cyclin D1 and CDK4 in MDA-MB-231 and T47D cells in 24 h treatment (Fig. 4C–D). It should be noted that in 48 h BME and BHE extracts exert similar potential to decrease cyclin D1 and CDK4 mRNA levels in MDA-MB-231 and T47D cells (Fig. 4C–D).

3.5. B. frutescens extracts increase mRNA levels of cell cycle regulator protein p21

To explore the modulatory role of cyclin D1 and CDK4 in the presence of BME and BHE extracts in MDA-MB-231 and T47D breast cancer cells we examined the mRNA levels of p21. p21 protein is a member of the cyclin kinase inhibitor family which downregulates the CDK4/6 signaling pathway. Hexane and methanolic extracts exert similar fold increase of p21 mRNA levels (3.2–3.6 fold) in MDA-MB-231 cells in 24 h treatment. In contrary, BME exerts potential increase (10 fold) in p21 mRNA levels in T47D cells in comparison to BHE extract treatment in T47D cells in 24 h (Fig. 4E). Lesser effect of BME and BHE extracts on p21 mRNA levels was observed in test cell lines in 48 h treatment.

3.6. Effect of B. frutescens extracts on MDA-MB-231 and T47D breast cancer cells nuclear morphology

To verify the presence of apoptotic cells, we examined the change in nuclear morphology by using Hoechst staining dye in *B. frutescens* hexane/methanol extract treated MDA-MB-231/T47D breast cells and respective controls (non-treated cells). A significant number of apoptotic cells were observed in BHE and BME treated MDA-MB-231 cells at sub IC_{50} concentration in 16 h treatment (Fig. 5A). The apoptotic cells nuclei were condensed and fragmented as revealed by the Hoechst 33342 nuclear-staining dye at 20× resolution. Deformed shape of the nucleus has appeared in the extracts treated cells compared to control cells at a higher resolution (100×). Similarly, BHE and BME treated T47D cells at sub IC_{50} concentration showed a significant number of apoptotic cells in 16 h treatment.

3.7. B. frutescens extracts decrease mRNA levels of survivin and Bcl2 anti-apoptotic proteins

Survivin and Bcl2 anti-apoptotic proteins are associated with breast cancer progression and poor prognosis. To explore the suppressive role of BME and BHE extract on anti-apoptotic proteins in MDA-MB-231 and T47D breast cancer cells, we examined the mRNA levels of survivin and Bcl2 gene. BME treatment (24 h) significantly reduced the mRNA levels of survivin and Bcl2 in MDA-MB-231 and T47D cells (Fig. 5C–D). In comparison to Bcl2, mRNA levels of survivin in BME treated MDA-MB-231 and T47D cells were highly reduced in 24 h treatment. 48 h BME treatment reduced the survivin and Bcl2 levels in MDA-MB-231 and T47D cells in comparison to control cells (Fig. 5C–D). BHE treatment showed an impressive reduction in survivin mRNA levels in MDA-MB-231 (in 24 h) and T47D (in 48 h) cells (Fig. 5E–F).

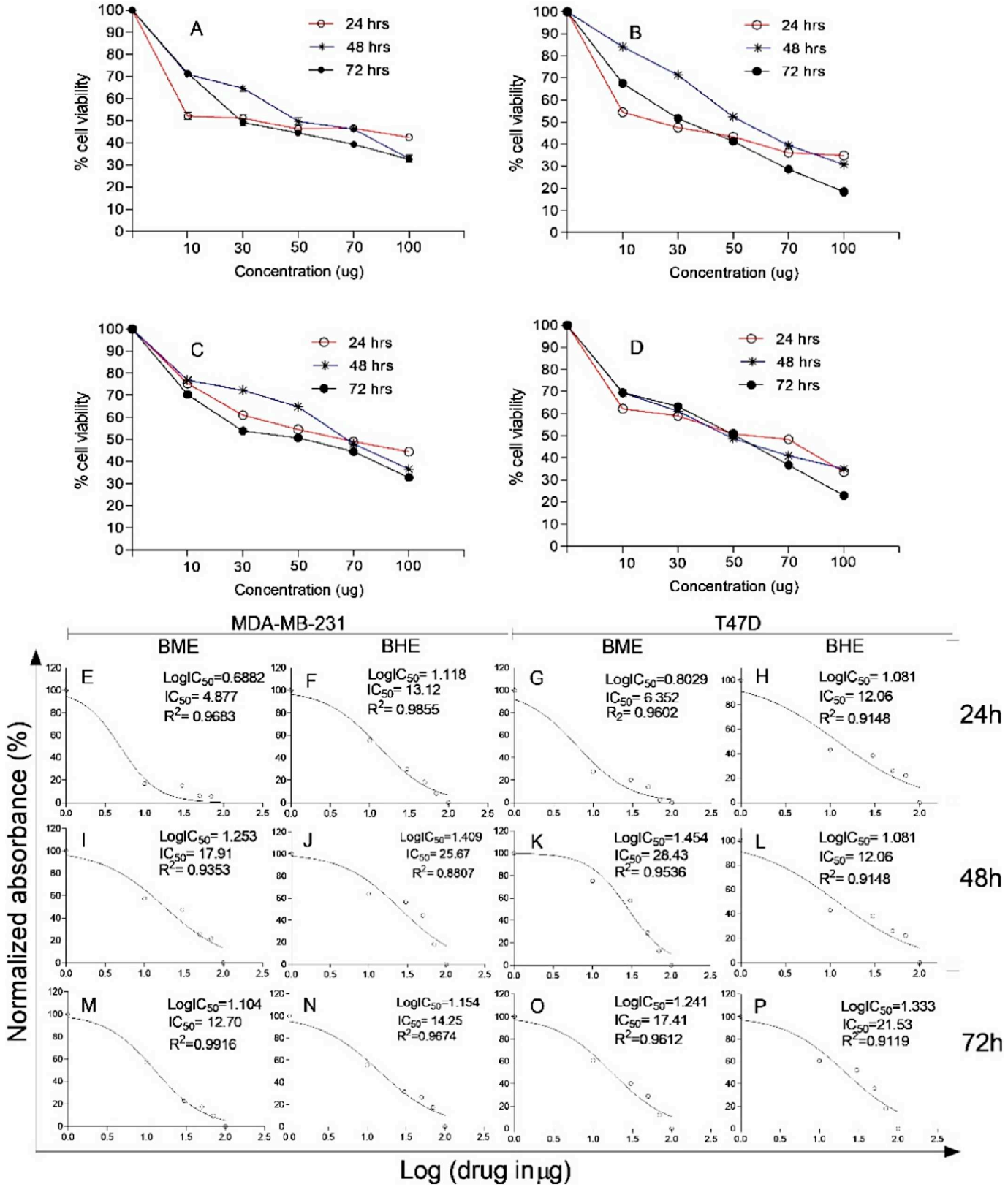

Fig. 2. Effect of *B. frutescens* extracts on human breast cancer cellular proliferation and regression analysis using MTT assay. (A) *B. frutescens* methanolic extract efficacy on MDA-MB-231 breast cancer cell proliferation. (B) *B. frutescens* methanolic extract efficacy on T47D breast cancer cell proliferation. (C) *B. frutescens* hexane extract efficacy on MDA-MB-231 breast cancer cell proliferation and (D) *B. frutescens* hexane extract efficacy on T47D breast cancer cell proliferation. (E)–(P) Representation of $IC_{50,}$ $LogIC_{50}$ values and regression analysis of the effect of BME and BHE extract (10, 30, 50, 70 and 100 µg/ml) in MDA-MB-231 and T47D cells in different time interval (24, 48 and 72 h) treatment. Results are expressed as mean ± SD.

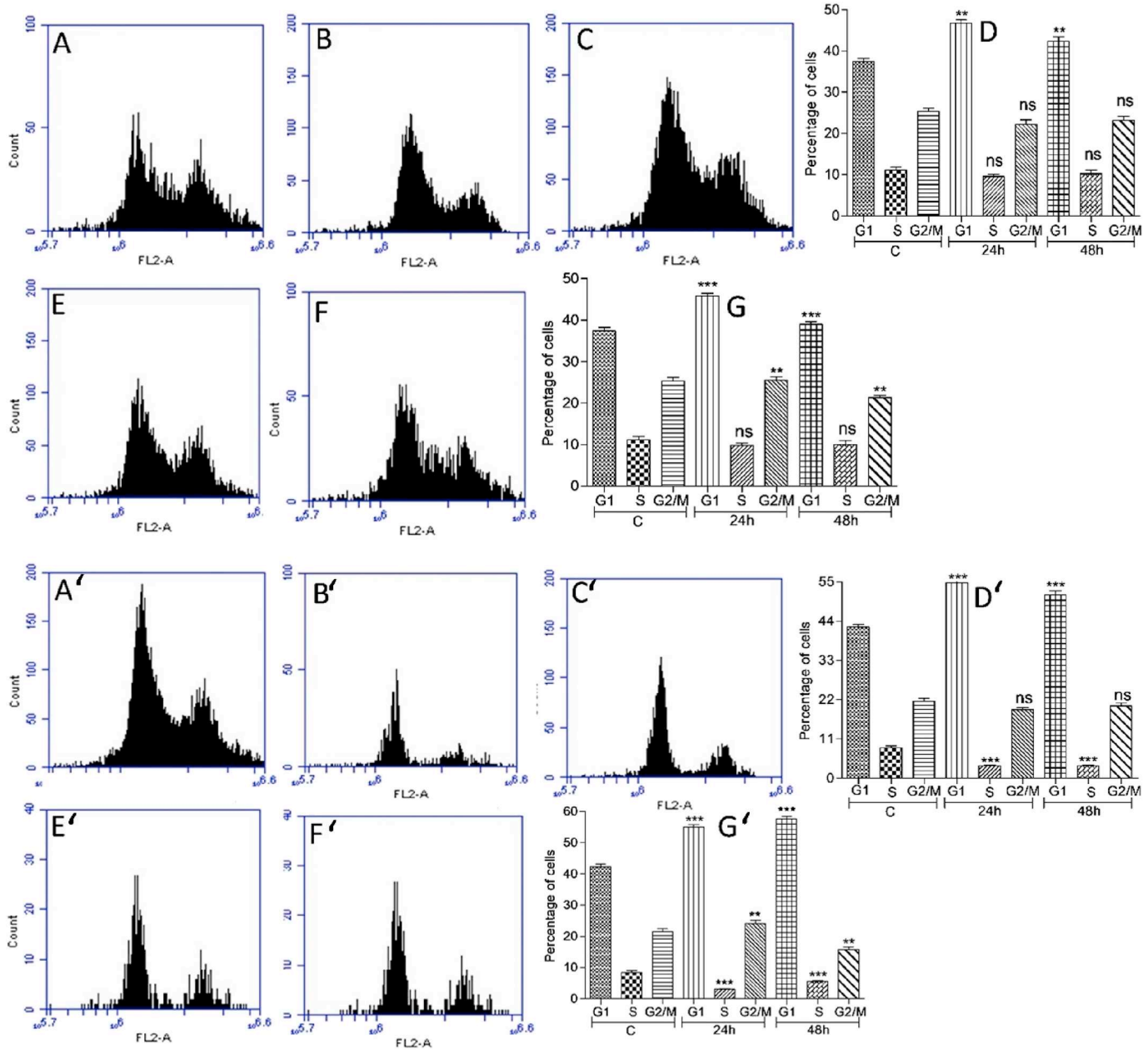

Fig. 3. Effect of *B. frutescens* extracts (BHE and BME) on cell cycle phase distribution in MDA-MB-231 and T47D breast cancer cell lines in 24 h and 48 h treatment at IC_{50} (A) Cell cycle phase distribution in untreated MDA-MB-231 cells. (B) and (C) *B. frutescens* methanolic extract efficacy on MDA-MB-231 cell cycle phase distribution in 24 h and 48 h of treatment respectively. (D) Graphical representation of the cell cycle phase distribution in untreated (A) and BME extract treated cells (B and C). (E) and (F) *B. frutescens* hexane extract efficacy on MDA-MB-231 cell cycle phase distribution in 24 h and 48 h of treatment respectively. (G) Graphical representation of the cell cycle phase distribution in untreated (A) and BHE extract treated cells (E and F).
(A′) Cell cycle phase distribution in untreated T47D cells. (B′) and (C′) *B. frutescens* methanolic extract efficacy on T47D cell cycle phase distribution in 24 h and 48 h of treatment respectively. (D′) Graphical representation of the cell cycle phase distribution in untreated (A′) and BME extract treated T47D cells (B′ and C′). (E′) and (F′) *B. frutescens* hexane extract efficacy on T47D cell cycle phase distribution in 24 h and 48 h of treatment respectively. (G′) Graphical representation of the cell cycle phase distribution in untreated (A′) and BHE extract treated cells (E′ and F′). Results are expressed as mean ± SD. ***$P < 0.0005$ vs. control; **$P < 0.005$ vs. control; *$P < 0.05$ vs. control.

3.8. B. frutescens extracts induce apoptosis in breast cancer cells at mRNA and protein level

To explore the inductive role of BME and BHE extracts on mitochondria-mediated apoptosis in MDA-MB-231 and T47D breast cancer cells we examined the mRNA levels of caspase 3. *B. frutescens* treatment showed significant fold increase (4.7–26 fold) of caspase 3 mRNA levels in MDA-MB-231 and T47D breast cells (Fig. 5I). Methanolic extract exerts time-dependent profound increase (23.22 fold) in caspase 3 mRNA levels in T47D cells after 48 h treatment. Hexane extract also depicted a significant increase (26 fold) in caspase 3 mRNA levels in MDA-MB-231 cells in 48 h treatment. In 48 h treatment with BME and BHE extracts in MDA-MB-231 and T47D cancer cells significant increase (20–26 fold) in caspase 3 level was observed (Fig. 5I). Comparatively better efficacy of extracts against MDA-MB-231 cells motivated us to study the procaspase expression at the protein level. Western blot analysis showed higher procaspase 3 protein level in extract-treated cells in comparison to non-treated breast cancer cells (Fig. 5J).

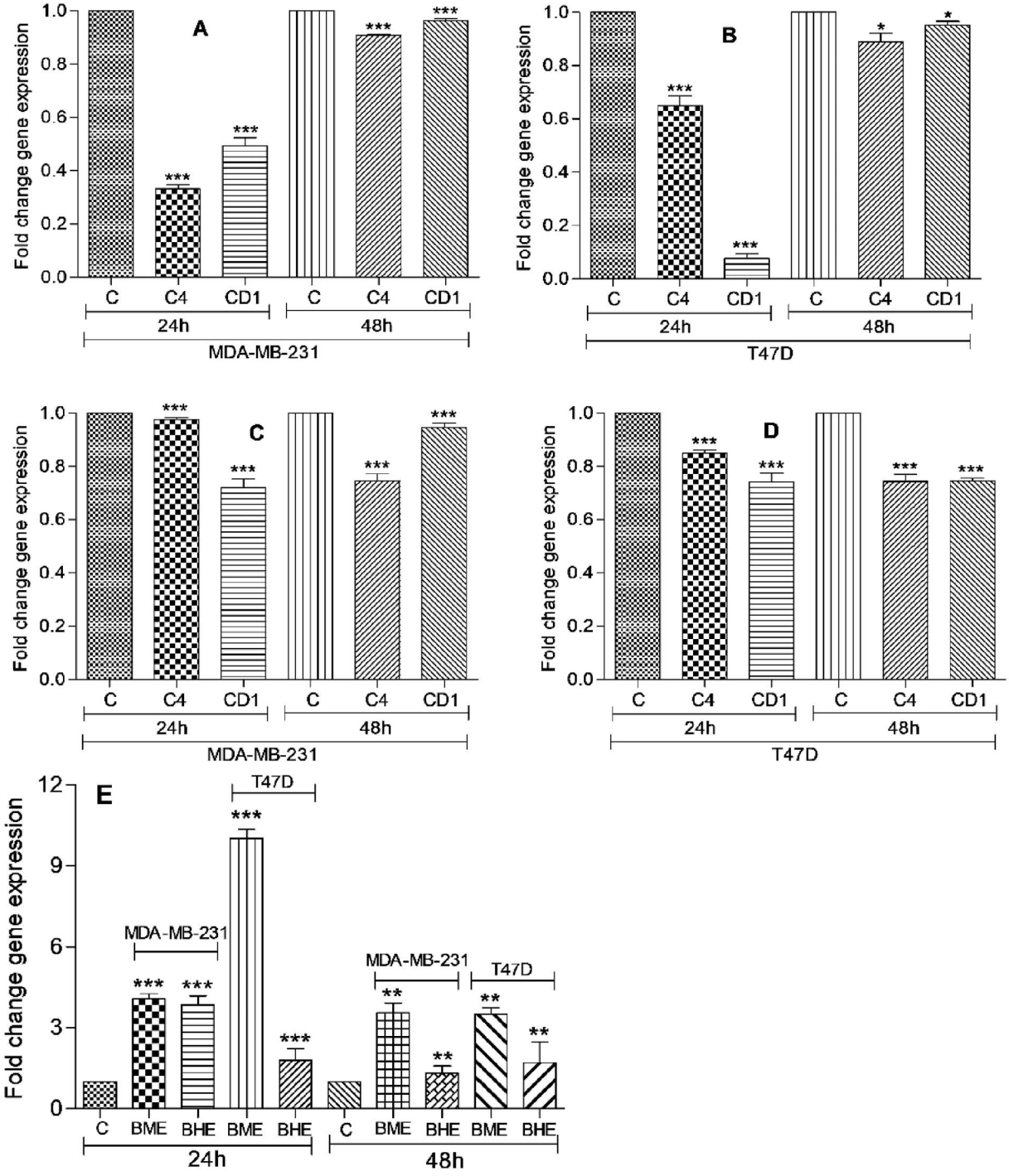

Fig. 4. Effect of *B. frutescens* extracts (BME and BHE) on mRNA levels of cell cycle markers (cyclin4, CD1 and p21) in human breast cancer cells proliferation at IC_{50} concentration for 24, and 48 h. (A) and (B) mRNA levels of CDK4 and cyclin D1 in *B. frutescens* methanolic extract treated MDA-MB-231 and T47D breast cancer cell respectively. (C) and (D) mRNA levels of CDK4 and cyclin D1 in *B. frutescens* hexane extract treated MDA-MB-231 and T47D breast cancer cell respectively. (E) p21 mRNA levels in *B. frutescens* methanol and hexane extract treated MDA-MB-231 and T47D breast cancer cell. Results are expressed as mean ± SD of the three replicates. ***$P < 0.0005$ vs. control; **$P < 0.005$ vs. control; *$P < 0.05$ vs. control. C = control; C4 = CDK4; CD1-Cyclin D1.

3.9. BME and BHE induces dose-dependent early apoptosis in breast cancer cells

B. frutescens extract showed better apoptotic inducing capacity (26 fold increase in caspase 3 mRNA level) in MDA-MB-231 cells (Fig. 5). Thus we quantified apoptosis induction ability of BHE and BME extract in 12 h treatment MDA-MB-231 breast cells using Annexin-V/PI double staining assay. The result showed that BHE and BME have little impact on late apoptosis (2–4%) at both sub IC_{50} and IC_{50} concentration. BHE treatment increased early apoptotic MDA-MB-231 cell population from ≈4% to ≈15% at sub IC_{50} and IC_{50} concentration respectively. BME treatment showed a 10% to 15% increase in early apoptotic cells at sub IC_{50} and IC_{50} concentration respectively in comparison to non-treated cells (Fig. 5H and H). It should be noted that BHE and BME treatment at IC_{50} in 12 h showed 6% breast cancer cell necrotic population.

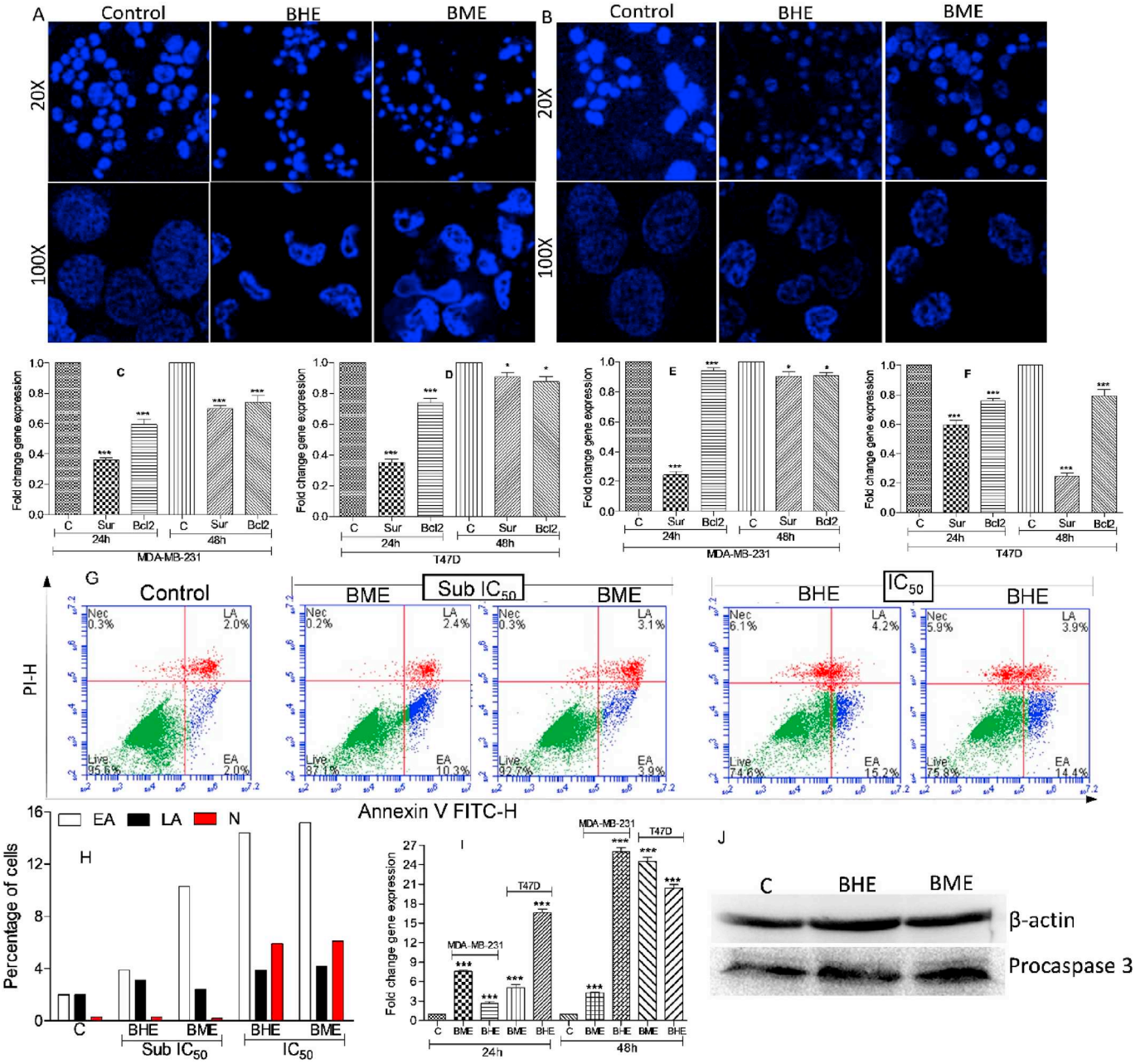

Fig. 5. Effect of *B. frutescens* extracts on apoptosis induction potential in breast cancer cells.

(A) and (B) Confocal microscopy was used to show the effect of *B. frutescens* extracts on nuclear morphology of MDA-MB-231 and T47D breast cells respectively using Hoechst dye at sub IC_{50} concentration.

RT-PCR technique was used to show the effect of *B. frutescens* extracts on mRNA levels of survivin, Bcl2 and caspase 3 markers in human breast cancer cells at IC_{50} concentration in 24, and 48 h treatment. (C) and (D) mRNA levels of survivin and Bcl-2 in *B. frutescens* methanolic extract treated MDA-MB-231 and T47D cells respectively. (E) and (F) mRNA levels of survivin and Bcl-2 in *B. frutescens* hexane extract treated MDA-MB-231 and T47D cells respectively.

Flow cytometry technique was used to quantify the *B. frutescens* extracts apoptosis induction potential in breast cancer cells. (G) BME and BHE induced apoptotic cell death in MDA-MB-231 breast cancer cells at sub IC_{50} and IC_{50} concentration in 12 h treatment. (H) Percentage representation of early apoptotic, late apoptotic and necrotic cell population in BME and BHE treated MDA-MB-231 cells in comparison to non-treated cells.

(I) mRNA levels of caspase 3 in *B. frutescens* methanolic and hexane extract treated MDA-MB-231 and T47D breast cancer cells.

Effect of *B. frutescens* extracts on procaspase 3 protein expression was studied in MDA-MB-231 cells using Western blot technique. The cell samples were collected after 12 h BME and BHE treatment at IC_{50} concentration. (J) Procaspase 3 protein expression in BHE and BME treated MDA-MB-231 cells. β-actin was used as an internal control.

Results are expressed as mean ± SD of the three replicates. $^{***}P < 0.0005$ vs. control; $^{**}P < 0.005$ vs. control; $^{*}P < 0.05$ vs. control. BHE = *B. frutescens* hexane extract; BME = *B. frutescens* methanol extract; PI-H = propidium iodide-height; EA = early apoptosis; LA = late apoptosis; N = necrosis; C = control.

3.10. Notch promoter activity

In order to elucidate the inhibitory potential of BME and BME on ϒ-secretase activity, we assessed the luciferase activity to check whether NICD is produced or not in the presence of test extracts. Inhibition of ϒ-secretase enzyme by inhibitors stops NICD production and thereby decrease downstream transcription of notch targeted genes. Non treated transfected cells showed luciferase gene transcription (Fig. 6B).

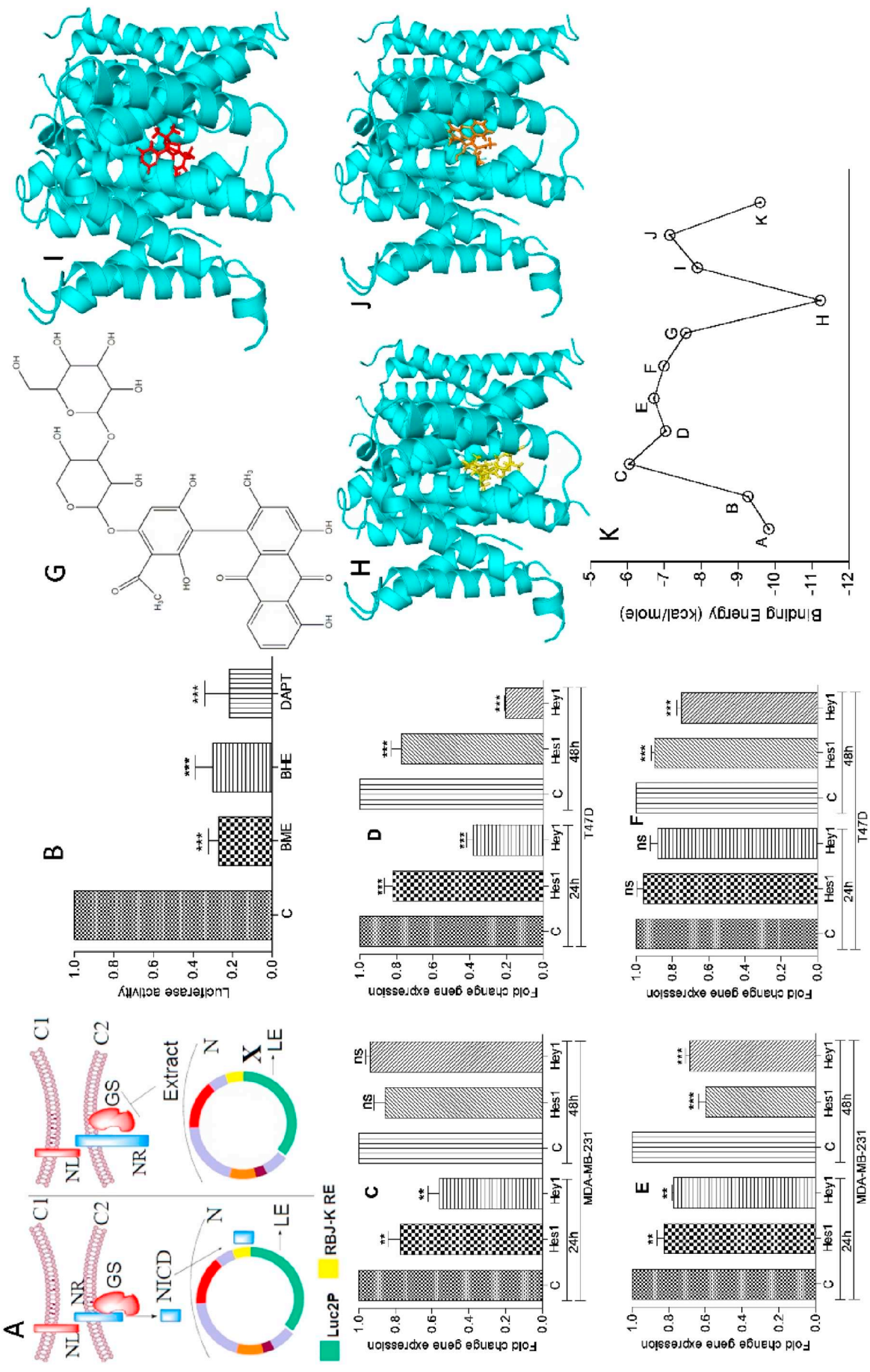
A
C1
C2
NL
NR
GS
NICD
N
LE
Luc2P
RBJ-K RE
Extract
X
B
Luciferase activity
C
BME
BHE
DAPT
G
H
I
J
K
Binding Energy (kcal/mole)
Fold change gene expression
Hes1
Hey1
24h
48h
MDA-MB-231
T47D
ns

Fig. 6. Notch signaling pathway inhibitory potential in *B. frutescens* extracts against breast cancer cells.
Notch dual luciferase promoter assay was used to study the notch signaling pathway inhibition by BHE and BME at promoter level. (A) Left and right panel shows activation and inhibition of notch signaling pathway respectively. In left panel, NICD is produced by notch-ligand interaction and activation of ϒ-secretase enzyme. Interaction of NICD to RBJ-K RE sequence (notch promoter sequence) initiates luciferase gene expression. Right panel shows inhibition of luciferase gene expression in the presence of *B. frutescens* phytochemicals which inhibits ϒ-secretase mediated NICD production. (B) Inhibitory potential of BME and BHE (IC_{50} concentration) extracts and standard notch inhibitor DAPT (20 μM) on notch promoter using dual luciferase assay. HEK293 cells were used for the experiment and luminescence was recorded on GloMax 20/20 Luminometer.
RT-PCR technique was used to show the effect of *B. frutescens* extracts on mRNA levels of notch responsive genes (Hes1 and Hey1) in MDA-MB-231 and T47D cells. The cells were treated at IC_{50} concentration for 24 and 48 h. (C) and (D) mRNA levels of Hes1 and Hey1 in BME treated MDA-MB-231 and T47D breast cancer cells respectively. (E) and (F) mRNA levels of Hes1 and Hey1 in BHE treated MDA-MB-231 and T47D breast cancer cells respectively.
Literature based identified *B. frutescens* phytochemicals were used for in silico docking study against ϒ-Secretase protein. Detailed methodology and software used for the study is given Methodology section. (G) 2D structure of the lead compound bulbineloneside D. (H) Interaction pattern of 4B5 ligand with ϒ-Secretase protein. (I) Interaction pattern of DAPT with ϒ-Secretase protein. (J) Interaction pattern of ϒ-Secretase with bulbineloneside D (PCID-10008440). (K) Binding energy score of different *B. frutescens* phytochemicals with ϒ-secretase protein. Alphabets A to K in the graph represent standard inhibitor and test ligands.
Results are expressed as mean ± SD of the three replicates. $^{***}P < 0.0005$ vs. control; $^{**}P < 0.005$ vs. control; $^{*}P < 0.05$ vs. control. NL = Notch ligand; NR = Notch receptor; C1 = cell membrane of cell 1; C2 = cell membrane of cell 2; GM = gamma secretase; NICD = Notch intracellular cleaved domain; N = nucleus; LE = luciferase expression; 4B5-N-{(2*R*,4*S*,5*S*)-2-benzyl-5-[(tert-butoxycarbonyl)amino]-4-hydroxy-6-phenylhexanoyl}-L-leucyl-L-phenylalaninamide; A-N-{(2*R*,4*S*,5*S*)-2-benzyl-5-[(tert-butoxycarbonyl)amino]-4-hydroxy-6-phenylhexanoyl}-L-leucyl-L-phenylalaninamide; B-DAPT; C-Isofuranonapthoquinone; D-Jozikniopholone A; E-Jozikniopholone B; F-Knipholone; G-Gaboroquinone B; H-bulbineloneside D; I-Gaboroquinone A; J-Isoknipholone; K-4′-demethylknipholone 2′-β-D-glucopyranoside.

Standard notch signaling and ϒ-secretase inhibitor DAPT was taken as control. Luciferase gene transcription was significantly decreased in BME, BHE and DAPT treated transfected-HEK293 cells. BME, BHE and DAPT treatment showed 3.7, 3.33, and 5 fold downregulation of luciferase gene expression in 24 h respectively (Fig. 6B).

3.11. B. frutescens extracts decrease mRNA levels of notch responsive Hes1 and Hey1 gene

To confirm the role of BME and BHE extract on notch signaling pathway in MDA-MB-231 (ER^-/PR^- breast cancer cell model) and T47D breast cancer cells, we examined the mRNA levels of notch responsive Hes1 and Hey1 gene. Notch signaling pathway upregulate in breast cancer. BME treatment significantly reduced the Hes1 and Hey1 mRNA levels in MDA-MB-231 and T47D cells in 24 h treatment (Fig. 6C and D). BME extract significantly reduced Hey1 mRNA levels (2.5 and 5 fold) in T47D cancer cells at 24 h and 48 h (Fig. 6D). Comparatively less effect of BME treatment was found on Hes1 and Hey1 mRNA levels in MDA-MB-231 cells in 48 h treatment (Fig. 6C). In comparison to BME extract, BHE treatment showed less potential to decrease the mRNA levels of Hes1 and Hey1 in MDA-MB-231 and T47D cells in 24 h and 48 h treatment (Fig. 6E and F).

3.12. B. frutescens extracts decreased mitochondrial membrane potential in confocal and spectrophotometric assays

To explore the mitochondria-mediated apoptosis induction potential of BME and BHE extracts in MDA-MB-231 and T47D breast cancer cells, we examined the disrupted mitochondrial membrane potential using confocal microscopy and spectrophotometry technique. JC-1 fluorescent dyes can gather in the mitochondrial matrix and produce red fluorescence. If the mitochondrial membrane potential is reduced, JC-1 cannot gather into the matrix and present as a monomer, producing green fluorescence. JC-1 fluorescent color changed from red to green in the BME and BHE treated MDA-MB-231 and T47D cell lines at sub IC_{50} concentration in 16 h, suggesting a decline in mitochondrial membrane potential (Fig. 7).

BME and BHE extract treatment at IC_{50} concentration in 48 h showed an appreciable decrease in mitochondrial membrane potential as revealed by increased fluorescence count (Fig. 7) in MA-MB-231 and T47D cells. Both the extracts showed approximately similar potential to decrease the membrane potential in both the test cell lines. Comparatively, the BHE extract depicted better membrane potential lowering effect in MDA-MB-231 and T47D cell than BME extract (Fig. 7).

3.13. B. frutescens extracts increased ROS production in confocal and spectrophotometric assays

To explore the possibility of ROS generation mediated mortality in MDA-MB-231 and T47D breast cancer cells in the presence of BME and BHE extracts, we examined the ROS production using confocal microscopy and fluorescence spectrophotometric technique using H2-DCFDA dye. Confocal microscopy with H2-DCFDA showed enhanced green fluorescence implying high ROS generation at sub IC_{50} concentration in 16 h. BME and BHE extract treatment at IC_{50} concentration in 48 h showed an appreciable increase in ROS generation as depicted by the increased fluorescence count (Fig. 8D) in MA-MB-231 and T47D cells. Both the extracts showed approximately similar efficacy to increase ROS generation independently in MA-MB-231 and T47D cell lines. Comparatively, the BHE extract depicted better ROS generation potential in both test cell lines (Fig. 8D). It should be noted that MDA-MB-231 breast cells produced more ROS in the presence of BME and BHE extracts in comparison to T47D cells (Fig. 8D).

3.14. B. frutescens extracts induce NF-κB mRNA levels in breast cancer cells

To explore the oxidative stress inductive role of BME and BHE extracts in MDA-MB-231 and T47D breast cancer cells we examined the mRNA levels of NF-κB. BME treatment in 24 h and 48 h show significant fold increase (1.9–9.3 fold) in NF-κB mRNA levels in MDA-MB-231 and T47D cells (Fig. 8C). Methanolic extract exerts time-dependent profound increase (5.1–9.3 fold increase) in NF-κB mRNA levels in MDA-MB-231 and T47D cells in 48 h. Hexane extract also depicted a significant increase in NF-κB mRNA levels in MDA-MB-231 cells in 48 h treatment in comparison to non-treated cells. It should be noted that in 48 h treatment with BHE extracts exceptionally showed decreased levels of NF-κB in both the MDA-MB-231 and T47D cells in 48 h than that of 24 h treatment (Fig. 8C).

3.15. In silico notch inhibitory potential of B. frutescens phytochemical

The γ-secretase enzyme is one of the important targets in the notch signaling pathway mediated natural anticancer drug discovery. Keeping this in our mind and based on in vitro down-regulated notch signaling pathway in *B. frutescens* treated breast cancer cells we tried to identify the potential notch inhibitor present in test extract. Methanol soluble phytochemicals in *B. frutescens* plant literature was surveyed as per methodology is given in the methods section. Isofuranonaphthoquinone, Jozikniopholone A, Jozikniopholone B, Knipholone, Isoknipholone, 4′-Demethylknipholone 4′-β-D-

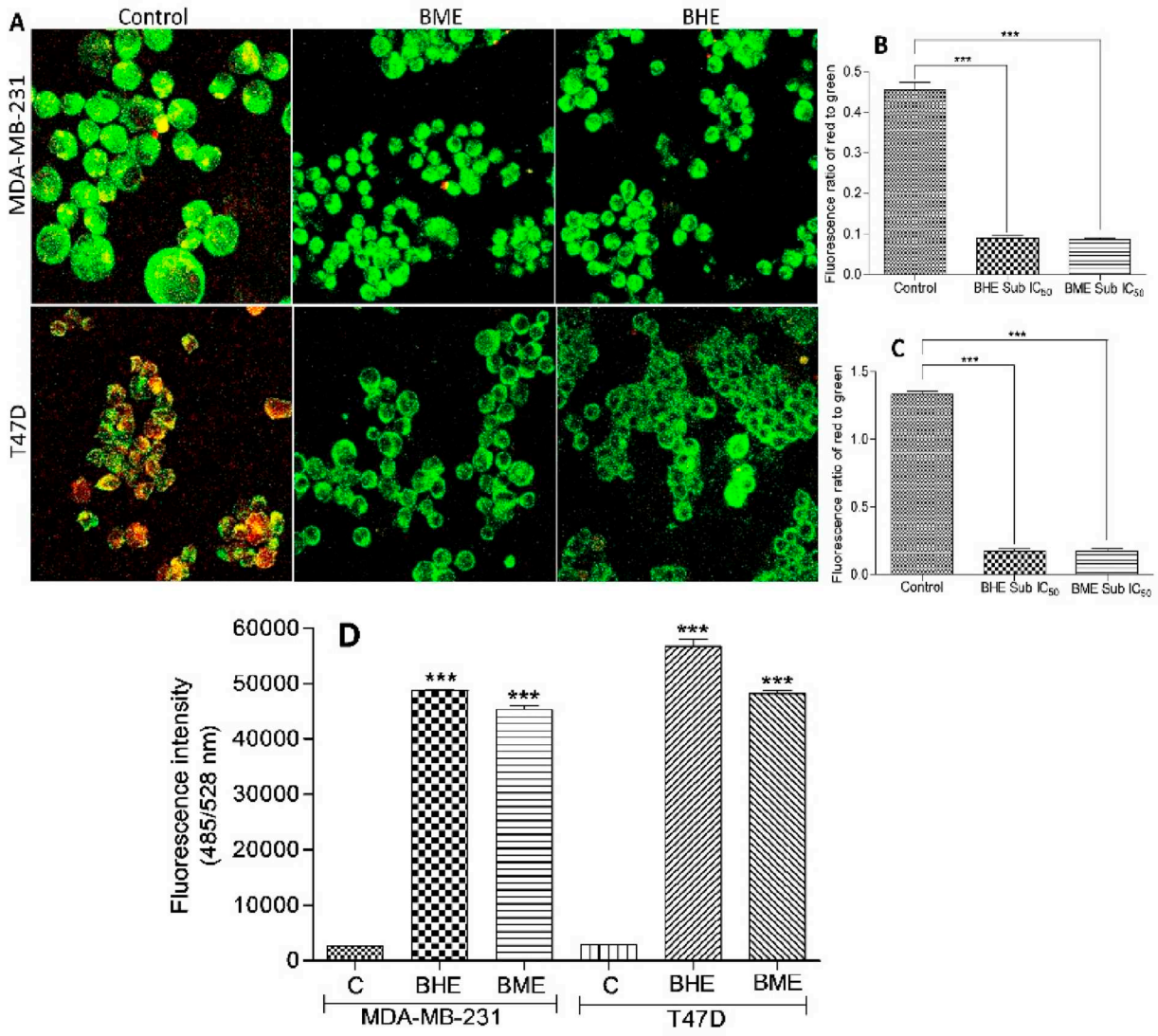

Fig. 7. Confocal microscopy and fluorescent spectroscopy showing effect of *B. frutescens* extracts on mitochondrial membrane potential in breast cells at sub IC_{50} and IC_{50} concentration.
(A) Effect of *B. frutescens* extracts on MDA-MB-231 and T47D cells. JC-1 fluorescent dye gathered in the matrix of mitochondria and produced red fluorescence in control sample. Due to decrease in mitochondrial membrane potential, JC-1 monomer produced green fluorescence in BME and BHE treated samples. (B) Graph showing the ratio of red and green fluorescence intensity in MDA-MB-231 cells. (C) Graph showing the ratio of red and green fluorescence intensity in T47D cells. (D) Effect of BME and BHE on MMP in human breast cancer cells at IC_{50} concentration in 48 h. BME = *B. frutescens* methanolic extract, BHE = *B. frutescens* hexane extract. Results are expressed as mean ± SD of the three replicates. ***$P < 0.0005$ vs. control; **$P < 0.005$ vs. control; *$P < 0.05$ vs. control. (For interpretation of the references to color in this figure legend, the reader is referred to the web version of this article.)

glucopyranoside, Gaboroquinones A, Gaboroquinones B, and Bulbineloneside D phytochemicals were identified as methanol soluble secondary metabolites in *B. frutescens* plant [19–22]. Co-crystalized (N-{(2*R*,4*S*,5*S*)-2-benzyl-5-[(tert-butoxycarbonyl)amino]-4-hydroxy-6-phenylhexanoyl}-L-leucyl-L-phenylalaninamide) and standard notch inhibitor (DAPT) were taken as positive control for in silico docking study. Co-crystalized and standard inhibitors showed approximately equal binding potential (−9.83 and −9.26 kcal/mol respectively) against γ-secretase enzyme binding pocket. Interestingly, bulbineloneside D from *B. frutescens* showed increased binding affinity (−11.22 kcal/mol) for ϒ-secretase compared to standard inhibitors (Fig. 6K). Further, in silico investigation showed the presence of hydrophobic interaction between bulbineloneside D and ϒ-secretase active site. Docking pose of standard and lead phytochemical is depicted in Fig. 6H–J. The ϒ-secretase amino acid residues and type of interaction with standards/lead compound are summarized in Table S3 in supplemental materials. The actual position of amino acid residues and their type of interaction with standard and lead compound is given in Fig. S1 in supplemental materials.

4. Discussion

Bulbine frutescens is a medicinal plant but very little is known about this plant till date. Some of the pharmacological activities such as anti-HIV and glutathione S-transferase inhibitory potential are reported [23]. The literature revealed the presence of quinones and glycoside in *B. frutescens* plant. These groups of secondary metabolites are potent anticancer agent [20]. Keeping this in our mind we studied the anticancer potential of *B. frutescens* plant and tried to deduce the possible anticancer mode of action. Aggressiveness, recurrence, and treatment of breast cancer depend upon the breast cancer subtypes. In the present study, triple-negative breast cancer (MDA-MB-231) and luminal (T47D) breast cancer cells were taken into consideration to assess the anticancer effect of *B. frutescens* extracts. In vitro anticancer screening of the

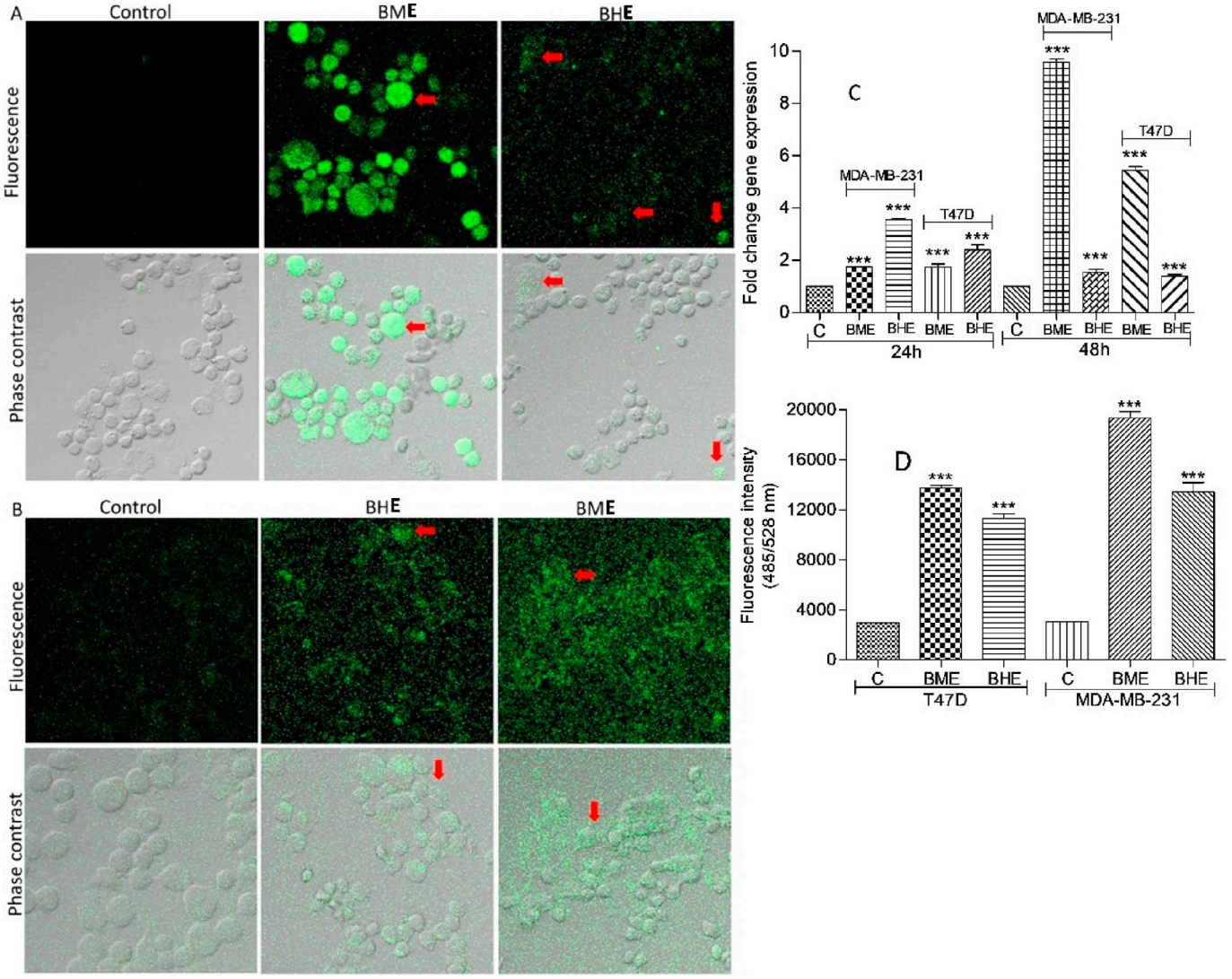

Fig. 8. Effect of BME and BHE extracts on ROS production and NF-κB mRNA levels in MDA-MB-231 and T47D cells.
(A) and (B) Confocal microscopy showing effect of *B. frutescens* extracts on ROS production in MDA-MB-231 and T47D breast cells respectively using H2-DCFDA dye at sub IC_{50} concentration. Confocal images of MDA-MB-231 and T47D cells showed enhanced fluorescence of CH-H2DCFDA which is directly proportional to cellular ROS. (C) Effect of *B. frutescens* extracts on mRNA levels of NF-κB marker in human breast cancer cells at IC_{50} concentration for 24 and 48 h in RT-PCR analysis. (D) Effect of *B. frutescens* extracts on ROS production in human breast cancer cells at IC_{50} concentration for 48 h. Results are expressed as mean ± SD of the three replicates. $^{***}P < 0.0005$ vs. control; $^{**}P < 0.005$ vs. control; $^{*}P < 0.05$ vs. control.

two *B. frutescens* extracts (BME and BHE) showed different potential against the test cell lines at different concentration and time interval treatment (Fig. 2). TNBC and luminal breast cancer cells show a difference in prognosis extent and chemotherapy response. It is reported that TNBC cells show poor prognosis and good chemotherapy response [24]. In the present study, we found that methanolic extract is more cytotoxic than hexane against both test cell lines at 24 h treatment (Fig. 2). BME and BHE treatment showed dose and time-dependent cytotoxicity in breast cancer cells (Fig. 2). The methanolic extract showed 2.69 and 1.89 times less IC_{50} than hexane extract against MDA-MB-231 and T47D cells at 24 h treatment respectively (Fig. 2). The difference in anticancer potential of the methanolic and hexane extracts of *B. frutescens* might be attributed to the differential occurrence of phytochemicals present in the respective extract (Fig. 1, Table S2 in supplemental materials). The potency of both (BME and BHE) extracts against the different origin of test breast cancer cells motivated us to study their mode of action in MDA-MB-231 and T47D cells.

Notch signaling activates with the interaction between Notch ligand and its receptor resulting in notch receptor cleavage by presenilin dependent ϒ-secretase enzyme. The cleaved notch intracellular domain (NICD) translocates to the nucleus and interacts with the transcription repressor complex. This interaction disperses the repressor complex machinery that presents on notch promoter and activates target gene (such as Hes1 and Hey1) transcription. Inhibition of the dispersal of promoter repressor complex machinery by targeting ϒ-secretase protein is one of the important mechanism to down-regulate the notch signaling pathway in cancer cells [25]. In the present study, we used Dual-Luciferase Reporter Assay to show the notch promoter inhibitory potential of test extracts. The result indicates that *B. frutescens* phytochemicals inhibited activation of notch promoter in extract-treated HEK293 cells (Fig. 6A–B). Moreover, results showed time-dependent downregulation of Hes1 and Hey1 genes in *B. frutescens* extract-treated T47D breast cells at mRNA levels (Fig. 6D). Thus BME and BHE extract have the potential to downregulate the Notch signaling pathway at the promoter level. Our in silico study revealed that lead phytochemical from *B. frutescens* extract (Bulbineloneside D) interact with ϒ-secretase protein is a similar way as the known standard notch inhibitor (DAPT). Moreover, the interaction of Bulbineloneside D with the two additional residues

(Ala80 and Leu81) provided stable binding (hydrophobic interaction) with the protein in comparison to DAPT. It may be inferred that *B. frutescens* phytochemicals have the potential to inhibit NICD formation by targeting ϒ-secretase enzyme.

The p21 (ubiquitous inhibitor of cyclin-dependent kinases), cyclin D1 and CDK4 (phosphorylate key cell cycle proteins) controls cell cycle at G1-S phase transition [26–28]. Notch signaling cascade regulates cell cycle by modulating the expression of cyclin D1, CDK4 and p21 levels in cancer cells [29]. Our results showed that *B. frutescens* extracts have the potential to arrest breast cancer cells in the G1 phase of the cell cycle (Fig. 3). BME and BHE extract upregulated p21 expression and downregulated Cyclin D1 and CDK4 at mRNA levels in breast cancer cells (Fig. 4). Decreased expression of caspase 3 and increased levels of anti-apoptotic protein (survivin and Bcl-2) is found in breast cancer cells [30]. Notch targeted genes are known to regulate apoptosis by modulating the activity/expression of caspase 3, survivin and Bcl2 proteins in breast cancer cells [31]. Chen et al. [32] reported that notch signaling upregulates survivin expression and thereby inhibit apoptosis in cancer cells [32]. Xia et al. [33] showed that treatment with phytochemical/extract downregulates notch signaling pathway and increases apoptotic: non-apoptotic protein ratio in breast cancer cells [33]. In the present study, BME and BHE treatment increased the cleaved caspase 3 fragment levels, suppressed Bcl-2 and survivin expression at mRNA level. Additionally, annexin V FITC and PI dual staining also confirmed the apoptotic induction potential in BHE and BME in triple-negative breast cancer cells (Fig. 5G and H). Increased levels of procaspase 3 protein in BHE and BME treated (12 h treatment) MDA-MB-231 cells substantiate the apoptotic induction potential of *B. frutescens* (Fig. 5J). Present study corroborate with the other findings which shows increased procaspase 3 protein levels in anticancer drug treated breast cancer cells [34]. Further, apoptosis induction potential of *B. frutescens* extract was confirmed by confocal microscopy. BME and BHE destroyed nuclear membrane, initiated cell shrinkage and membrane blebbing in treated breast cancer cells (Fig. 5). The present study is corroborated with a previous study which showed the formation of apoptotic bodies, nuclei condensation and fragmentation into segregated bodies in drug-treated cancer cells [35].

Reactive oxygen species are directly linked with the progression and aggressiveness of cancer. Cancer cells upregulate their antioxidant defense system to mitigate the adverse effect of elevated ROS levels up to a limit. Moreover, the energy requirement is also high in cancer cells which necessitate the presence of healthy mitochondria. Thus anticancer drugs that generate an excess of ROS and disrupt the structural integrity of mitochondria in cancer cells are of greater importance nowadays [36]. Excessive ROS production and alteration in mitochondrial membrane potential is associated with apoptosis initiation in breast cancer cells [36]. Data showed that BME extract induced 4.5 and 6.5 times ROS production in T47D and MDA-MB-231 cells respectively in comparison to non-treated cells. In contrary, both extracts showed greater mitochondrial membrane potential damage in T47D breast cells. Both, fluorescence spectroscopy and confocal microscopy techniques confirmed excessive ROS production and mitochondria membrane potential alteration in extract-treated breast cancer cells (Figs. 7–8).

5. Conclusion

In conclusion, *B. frutescens* polar (methanolic) and non-polar (hexane) extracts comprise of secondary metabolites having antiproliferative potential at microgram concentrations (IC_{50} 4–12 μg/ml). In best of own knowledge, this is the first statement on the therapeutic effect of *B. frutescens* on human breast cancer cells. *B. frutescens* have the potential to induce ROS production and apoptosis, and disrupt mitochondria membrane potential in TNBC (MDA-MB-231) and luminal (T47D) cells. *B. frutescens* phytochemicals combat breast cancer cell aggressiveness by downregulating the notch signaling pathway and arresting the cell cycle. In silico study revealed Bulbineloneside D as a novel ϒ-secretase enzyme inhibitor, that might responsible for the downregulation of the notch pathway in breast cancer cells. A further in-depth study is required to validate in vivo anticancer potential of *B. frutescens* extracts in order to render its effective therapeutic strategy against breast cancer. Limited availability of anticancer drugs and naturally occurrence of *B. frutescens* makes it a robust choice for future research endeavors.

Supplementary data to this article can be found online at https://doi.org/10.1016/j.lfs.2019.116783.

Declaration of competing interest

The authors declare no conflict of interest.

Acknowledgments

PPK acknowledges financial support from the University Grants Commission, India in the form of CSIR-UGC Senior Research fellowship. SK acknowledges University Grants Commission, India and Department of Science and Technology, India for providing financial support in the form of UGC-BSR Research Start-Up-Grant [No. F.30–372/2017 (BSR)] and DST-SERB Grant [EEQ/2016/000350] respectively. SK acknowledges Central University of Punjab, Bathinda, India for providing Research Seed Money Grant [GP-25]. AKS, SKP, and MS acknowledge CSIR-India, DBT-India and DST-India funding agencies respectively for providing financial assistance in the form of Junior Research Fellowship.

References

[1] F. Bray, J. Ferlay, I. Soerjomataram, R.L. Siegel, L.A. Torre, A. Jemal, Global cancer statistics 2018: GLOBOCAN estimates of incidence and mortality worldwide for 36 cancers in 185 countries, CA Cancer J. Clin. 68 (6) (2018) 394–424.
[2] S. Kumar, A.K. Pandey, Medicinal attributes of *S. xanthocarpum* fruit consumed by several tribal communities as food: An antioxidant, anticancer and anti-HIV perspective, BMC Comp. Alt. Med. 14 (2014) 1–8.
[3] S. Kumar, G. Chashoo, A.K. Saxena, A.K. Pandey, *Parthenium hysterophorus*: a probable source of anticancer, antioxidant and anti-HIV agent, Biomed. Res. Int. 2013 (2013) 1–11.
[4] E.W. Mollen, J. Ient, V.C. Tjan-Heijnen, L.J. Boersma, L. Miele, M.L. Smidt, et al., Moving breast cancer therapy up a Notch, Front. Oncol. 8 (2018) 1–25.
[5] Q. Zhang, Y. Yuan, J. Cui, T. Xiao, D. Jiang, Paeoniflorin inhibits proliferation and invasion of breast cancer cells through suppressing Notch-1 signaling pathway, Biomed. Pharmacother. 78 (2016) 197–203.
[6] S.R. Oakes, F. Vaillant, E. Lim, L. Lee, K. Breslin, F. Feleppa, et al., Sensitization of BCL-2–expressing breast tumors to chemotherapy by the BH3 mimetic ABT-737, Proc. Natl. Acad. Sci. 109 (8) (2012) 2766–2771.
[7] B. Cohen, M. Shimizu, J. Izrailit, N.F. Ng, Y. Buchman, J.G. Pan, et al., Cyclin D1 is a direct target of JAG1-mediated Notch signaling in breast cancer, Breast Cancer Res. Treat. 123 (1) (2010) 113–124.
[8] Z. Lu, Y. Ren, M. Zhang, T. Fan, Y. Wang, Q. Zhao, G. Hou, FLI-06 suppresses proliferation, induces apoptosis and cell cycle arrest by targeting LSD1 and Notch pathway in esophageal squamous cell carcinoma cells, Biomed. Pharmacother. 107 (2018) 1370–1376.
[9] N.R. Gough, Notch protects the mitochondria, Sci. Signal. 3 (118) (2010) (ec119-ec119).
[10] N. Pather, B. Kramer, *Bulbine Natalensis* and *Bulbine Frutescens* promote cutaneous wound healing, J. Ethnopharmacol. 144 (3) (2012) 523–532.
[11] M. van Huyssteen, P.J. Milne, E.E. Campbell, M. van de Venter, Antidiabetic and cytotoxicity screening of five medicinal plants used by traditional African health practitioners in the Nelson Mandela Metropole, South Africa, Afr. J. Tradit. Complement. Altern. Med. 8 (2) (2011) 150–158.
[12] S. Mukanganyama, M. Bezabih, M. Robert, B.T. Ngadjui, G.F. Kapche, F. Ngandeu, et al., The evaluation of novel natural products as inhibitors of human glutathione transferase P1-1, J. Enzyme Inhib. Med. Chem. 26 (4) (2011) 460–467.
[13] T. Mosmann, Rapid colorimetric assay for cellular growth and survival: application to proliferation and cytotoxicity assays, J. Immunol. Methods 65 (1–2) (1983) 55–63.
[14] R.J. White, I.J. Reynolds, Mitochondrial depolarization in glutamate-stimulated neurons: an early signal specific to excitotoxin exposure, J. Neurosci. 16 (18) (1996) 5688–5697.
[15] D. Wu, P. Yotnda, Production and detection of reactive oxygen species (ROS) in cancers, J. Vis. Exp. 57 (2011) 1–4.
[16] Z. Darzynkiewicz, G. Juan, DNA content measurement for DNA ploidy and cell cycle analysis, Curr. Protoc. Cytom. 00 (2001) (7.5:7.5.1–7.5.24).
[17] D. Wlodkowic, J. Skommer, Z. Darzynkiewicz, Flow cytometry-based apoptosis detection, Methods Mol. Biol. 559 (2009) 1–14.
[18] H. Mechoulam, E.A. Pierce, Expression and activation of STAT3 in ischemia-

induced retinopathy, Invest. Ophthalmol. Vis. Sci. 46 (12) (2005) 4409–4416.
[19] G. Bringmann, J. Mutanyatta-Comar, K. Maksimenka, J.M. Wanjohi, M. Heydenreich, R. Brun, Joziknipholones A and B: the first dimeric phenylanthraquinones, from the roots of *Bulbine frutescens*, Chem. Eur. J. 14 (5) (2008) 1420–1429.
[20] P. Tambama, B. Abegaz, S. Mukanganyama, Antiproliferative activity of the isofuranonaphthoquinone isolated from *Bulbine frutescens* against jurkat T cells, Biomed. Res. Int. 2014 (2014) 1–14.
[21] B.M. Abegaz, M. Bezabih, T. Msuta, R. Brun, D. Menche, J. Mühlbacher, Gaboroquinones A and B and 4′-O-demethylknipholone-4′-O-β-d-glucopyranoside, phenylanthraquinones from the roots of *Bulbine frutescens*, J. Nat. Prod. 65 (8) (2002) 1117–1121.
[22] M. Kuroda, Y. Mimaki, H. Sakagami, Y. Sashida, Bulbinelonesides A–E, phenylanthraquinone glycosides from the roots of *Bulbinella floribunda*, J. Nat. Prod. 66 (6) (2003) 894–897.
[23] R. Shikalepo, C. Mukakalisa, M. Kandawa-Schulz, W. Chingwaru, P. Kapewangolo, In vitro anti-HIV and antioxidant potential of *Bulbine frutescens* (Asphodelaceae), J. Herbal Med. 12 (2018) 73–78.
[24] S.J. Isakoff, Triple negative breast cancer: role of specific chemotherapy agents, Cancer J. 16 (1) (2010) 53–61.
[25] R. Olsauskas-Kuprys, A. Zlobin, C. Osipo, Gamma secretase inhibitors of notch signaling, Onco Targets Ther. 6 (2013) 943–955.
[26] C. Lange, W.B. Huttner, F. Calegari, Cdk4/cyclinD1 overexpression in neural stem cells shortens G1, delays neurogenesis, and promotes the generation and expansion of basal progenitors, Cell Stem Cell 5 (3) (2009) 320–331.
[27] S. Waga, G.J. Hannon, D. Beach, B. Stillman, The p21 inhibitor of cyclin-dependent kinases controls DNA replication by interaction with PCNA, Nature 369 (6481) (1994) 574–578.
[28] Y. Xiong, G.J. Hannon, H. Zhang, D. Casso, R. Kobayashi, D. Beach, p21 is a universal inhibitor of cyclin kinases, Nature 366 (6456) (1993) 701–704.
[29] M.Y. Dai, F. Fang, Y. Yi, X. Zou, Y.J. Ding, C. Chen, et al., Downregulation of Notch1 induces apoptosis and inhibits cell proliferation and metastasis in laryngeal squamous cell carcinoma, Oncol. Rep. 34 (6) (2015) 3111–3119.
[30] M. Xue, Y. Ge, J. Zhang, Q. Wang, L. Hou, Y. Liu, Q. Li, Anticancer properties and mechanisms of fucoidan on mouse breast cancer in vitro and in vivo, PLoS One 7 (8) (2012) 1–9.
[31] Z. Sun, C. Zhou, F. Liu, W. Zhang, J. Chen, Y. Pan, Q. Wang, Inhibition of breast cancer cell survival by xanthohumol via modulation of the Notch signaling pathway in vivo and in vitro, Oncol. Lett. 15 (1) (2018) 908–916.
[32] X. Chen, N. Duan, C. Zhang, W. Zhang, Survivin and tumorigenesis: molecular mechanisms and therapeutic strategies, J. Cancer 7 (3) (2016) 314–323.
[33] S. Xia, X. Zhang, C. Li, H. Guan, Oridonin inhibits breast cancer growth and metastasis through blocking the Notch signaling, Saudi Pharm. J. 25 (4) (2017) 638–643.
[34] J. Li, Q. Wang, Z. Wang, N. Cui, B. Yang, W. Niu, H. Kuang, Tetrandrine inhibits colon carcinoma HT-29 cells growth via the Bcl-2/caspase 3/PARP pathway and G1/S phase, Biosci. Rep. 39 (5) (2019) 1–12.
[35] S.A. Rahman, S. Nur, N. Abdul Wahab, A. Malek, S. Nurestri, In vitro morphological assessment of apoptosis induced by antiproliferative constituents from the rhizomes of *Curcuma zedoaria*, Evid. Based Complementary Altern Med. 2013 (2013) 1–14.
[36] M.L. Boland, A.H. Chourasia, K.F. Macleod, Mitochondrial dysfunction in cancer, Front. Oncol. 3 (2013) 1–28.